RSC Advances

PAPER

View Article Online
View Journal | View Issue

CrossMark click for updates

Cite this: *RSC Adv.*, 2016, **6**, 10683

# Multivalent photo-crosslinkable coumarin-containing polybenzoxazines exhibiting enhanced thermal and hydrophobic surface properties†

Ruey-Chorng Lin,[a] Mohamed Gamal Mohamed,[a] Kuo-Chih Hsu,[a] Jia-Yu Wu,[a] Yu-Ru Jheng[a] and Shiao-Wei Kuo*[ab]

In this study, mono-, bi-, and trivalent coumarin-containing benzoxazine monomers (mono-, di-, and tri-coumarin BZ) were synthesized in high yield and purity by facile Mannich reactions of 4-methyl-7-hydroxycoumarin and paraformaldehyde with aniline, bisphenol A–$NH_2$, and 1,3,5-tri(4-aminobenzene), respectively, in 1,4-dioxane. $^1$H and $^{13}$C nuclear magnetic resonance (NMR), Fourier transform infrared (FTIR) and high resolution mass spectroscopy support the chemical structures of these three benzoxazine monomers. Differential scanning calorimetry (DSC) and FTIR spectroscopy were used to investigate the curing polymerization behavior and photodimerization ([2π + 2π] cycloaddition) of the coumarin units of mono-, di-, and tri-coumarin BZ to form poly(mono-coumarin BZ), poly(di-coumarin BZ), and poly(tri-coumarin BZ), respectively. DSC measurement revealed that the thermal polymerization temperature of coumarin-containing benzoxazine monomers was lower than that of the model compound 3-phenyl-3,4-dihydro-2*H*-benzooxazine (263 °C) which was attributed to the catalytic effect of the coumarin moiety and a strong electron withdrawing electron conjugated C=C bond in the coumarin unit. In addition, the glass transition and thermal decomposition temperatures of poly(tri-coumarin BZ) ($T_g$ = 240 °C; $T_{d5}$ = 370 °C) were higher than poly(di-coumarin BZ) and poly(mono-coumarin BZ), consistent with the former's higher crosslinking density. In addition, the water contact angles of poly(tri-coumarin BZ) polymers prepared with and without photo-dimerization prior to thermal curing (112 and 110°, respectively) were higher than the corresponding poly(mono-coumarin BZ) and poly(di-coumarin BZ), presumably because of greater degrees of intramolecular hydrogen bonding between the C=O units of the coumarin moieties and the phenolic OH units of the benzoxazine rings, resulting in lower surface free energies. Thus, the presence of multivalent photo-crosslinkable coumarin units enhanced the thermal and hydrophobic surface properties of these polybenzoxazines.

Received 25th December 2015
Accepted 18th January 2016

DOI: 10.1039/c5ra27705a

www.rsc.org/advances

Published on 21 January 2016. Downloaded by Universitaet Osnabrueck on 29/01/2016 03:31:33.

## Introduction

Polybenzoxazines (PBZs) are phenolic resin polymers that have attracted much interest because of their ready synthesis (through thermal polymerization of benzoxazine monomers without the need for any catalysts)[1–5] and excellent properties (high thermal stability, good molecular design flexibility, chemical resistance, mechanical robustness, low flammability, and low surface free energy).[6–13] Nevertheless, many challenges must be overcome to enhance the processibility of these materials, which generally exhibit high melting and curing temperatures.[14–16]

The physical characteristics of PBZs can be modified in several ways (*e.g.*, introduction of nitrile, allyl, acetylene, or propargyl side groups, or strong hydrogen bonding moieties, on the benzoxazine monomers) to form interesting materials displaying varied thermal and mechanical properties and resistance to solvents.[17–20] The physical properties of PBZs (*e.g.*, their hydrophobic surface properties) are strongly dependent on the degrees of intramolecular hydrogen bonding between the phenolic hydroxyl (OH) groups and N atoms in the Mannich bridge and intermolecular OH···O hydrogen bonding (after ring opening of the benzoxazine monomers).[21]

Light-responsive groups are attractive materials that can change the behavior of their chromophores upon photo-irradiation, either through changes in their molecular structures or through the effects of different light sources.[22–25] Readily accessible photoresponsive molecules include spiropyran, diarylethene, stilbene, azobenzene, anthracene, cinnamic acids,

[a]*Department of Materials and Optoelectronic Science, National Sun Yat-Sen University, Kaohsiung, Taiwan. E-mail: kuosw@faculty.nsysu.edu.tw*

[b]*Department of Medicinal and Applied Chemistry, Kaohsiung Medical University, Kaohsiung, Taiwan*

† Electronic supplementary information (ESI) available: FTIR spectra, DSC traces, high resolution mass spectroscopy and WCAs of mono-coumarin BZ, di-coumarin BZ, and tri-coumarin BZ. This material is available free of charge *via* the internet. See DOI: 10.1039/c5ra27705a

Published on 21 January 2016. Downloaded by Universitaet Osnabrueck on 29/01/2016 03:31:33.

and cinnamic esters and coumarin derivatives. As known the photo-dimerization of coumarin unit and its derivatives in solution and solid state under photo-irradiation (350 nm) has been reported.[23,24] For example, the photo-irradiation of coumarin molecule in non-polar benzene afforded a mixture of *syn*-head-head, *anti*-head-head, *syn*-head-tail and *anti*-head-tail of cyclobutane dimers through $[2\pi + 2\pi]$ cycloaddition. In addition, the photocycloaddition reaction of coumarin unit is reversible when irradiated at a shorter wavelength (250 nm).[26–28] For example, Saegusa *et al.* investigated the reversible gelation of polyoxazolines with coumarin units.[29] Yagci *et al.* were the first to report the incorporation of coumarin units into benzoxazine structures, which exhibited high thermal stability after photo-dimerization of their coumarin moeities.[30] In addition, we previously synthesized a bifunctional benzoxazine monomer featuring pyrene and coumarin moieties; the glass transition temperature ($T_g$) increased after photo-dimerization of coumarin units, with the pyrene moieties enhancing the dispersion of single-walled carbon nanotubes through π–π stacking.[31]

In this present study, we prepared three new mono-, bi-, and trivalent coumarin/benzoxazine derivatives and converted them into photo-crosslinkable coumarin-containing PBZs in high yield and high purity (Scheme 1). We characterized these chemical structures using differential scanning calorimetry (DSC), thermogravimetric analysis (TGA), Fourier transform infrared (FTIR), nuclear magnetic resonance (NMR) and high resolution mass spectroscopy. In addition, we used DSC and FTIR spectroscopy to monitor the thermal curing polymerization of the monomers and the subsequent photo-dimerization of the coumarin units. Finally, we used water contact angle (WCA) measurements to examine the surface properties of these novel coumarin-functionalized benzoxazines before and after thermal curing at various temperatures.

## Experimental section

### Materials

Paraformaldehyde (96%), sodium bicarbonate ($NaHCO_3$), potassium carbonate ($K_2CO_3$), sodium hydroxide (NaOH), bisphenol A, resorcinol, ethyl acetoacetate, and ethyl acetate (EA) were purchased from Acros. 4-Chloro-4-nitrobenzene, 4-fluore-4-nitrobenzene, pyridine, and phloroglucinol (1,3,5-trihydroxybenzene) were purchased from Scharlau. Palladium on activated carbon (Pd/C) and hydrazine monohydrate (98%) were purchased from Alfa Aesar. Tetrahydrofuran (THF), *N*,*N*-dimethylformamide (DMF), 1,4-dioxane, chloroform ($CHCl_3$), dichloromethane

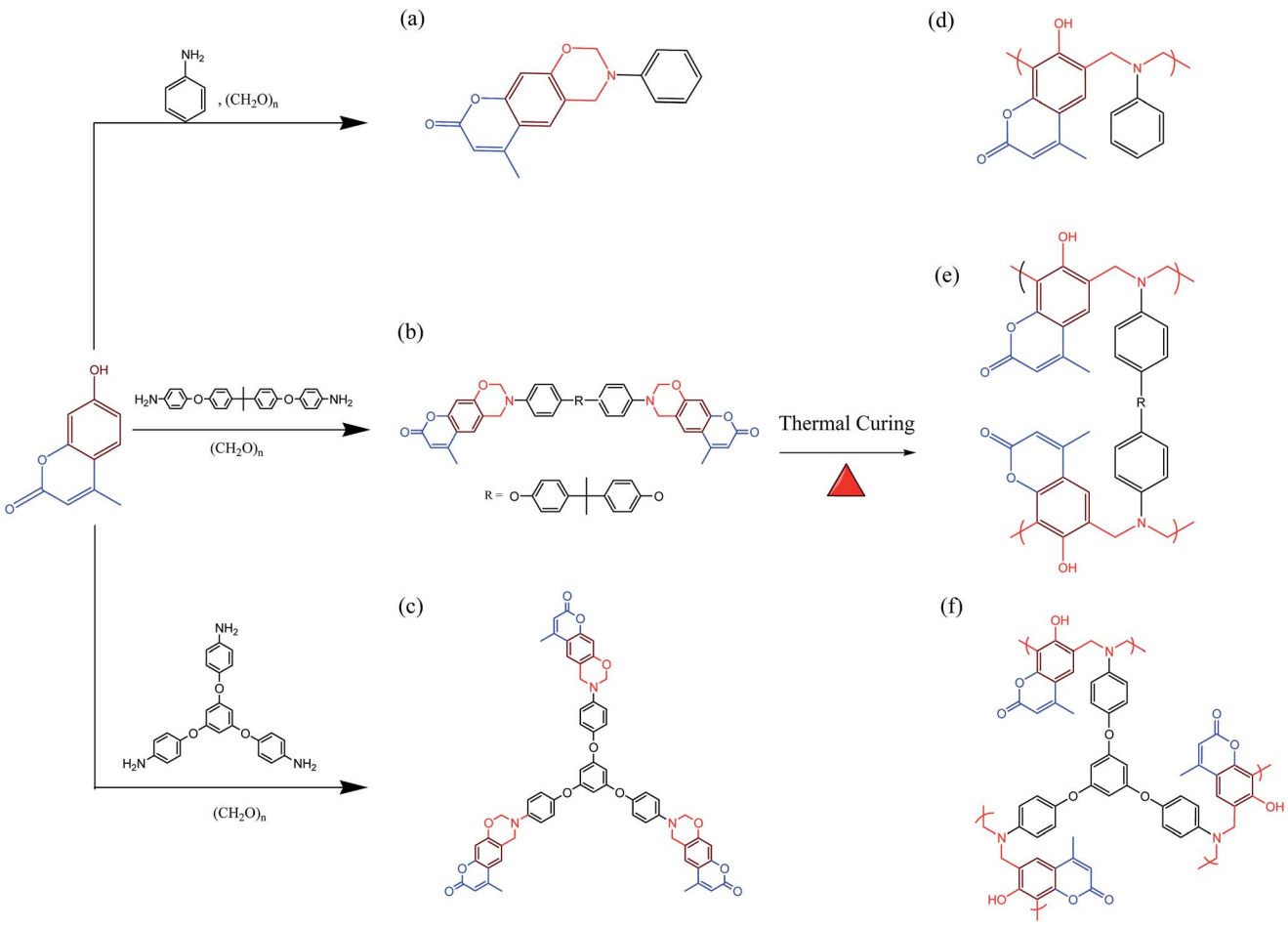


Scheme 1 Synthesis of (a) mono-coumarin BZ, (b) di-coumarin BZ, and (c) tri-coumarin BZ, and their thermal curing to form (d) poly(mono-coumarin BZ), (e) poly(di-coumarin BZ), and (f) poly(tri-coumarin BZ).

 This journal is © The Royal Society of Chemistry 2016

Published on 21 January 2016. Downloaded by Universitaet Osnabrueck on 29/01/2016 03:31:33.

($CH_2Cl_2$), and ethanol (EtOH) were purchased from Acros. 4-Methyl-7-hydroxycoumarin (coumarin–OH) was synthesized according to a previously reported procedure.[31]

**2,2-Bis(4-(4-nitrophenoxy)-phenyl)propane (bisphenol A–$NO_2$) (Scheme S1†).** A mixture of bisphenol A (3.00 g, 13.1 mmol), 1-chloro-4-nitrobenzene (4.35 g, 27.6 mmol), and $K_2CO_3$ (7.27 g, 52.6 mmol) in DMF (150 mL) was stirred under reflux (130 °C) under a $N_2$ atmosphere. After 48 h, the mixture was cooled and filtered the insoluble salts. The filtrate was evaporated to dryness under reduced pressure and the residue was then extracted with $CH_2Cl_2$ (3 × 80 mL). The combined extracts were washed several times with distilled water, dried ($MgSO_4$, 30 min), and concentrated. The solid product was recrystallized (EtOH), giving yellow crystals (2.62 g, 87%): mp (DSC): 122 °C. FTIR (KBr, $cm^{-1}$): 1587 and 1350 ($NO_2$ stretch). $^1$H NMR (500 MHz, DMSO-$d_6$, $\delta$, ppm): 7.10–8.25 (m, CH aromatic). $^{13}$C NMR (125 MHz, DMSO-$d_6$, $\delta$, ppm): 30.68 [$C(CH_3)_2$], 117.90–163.71 (aromatic).

**4-(4-(2-(4-(4-Aminosphenoxy)phenyl)propan-2-yl) phenoxy) benzenamine (bisphenol A–$NH_2$) (Scheme S1†).** A stirred mixture of bisphenol A–$NO_2$ (2.50 g, 5.32 mmol) and 10% Pd/C (0.033 g, 0.314 mmol) in absolute EtOH (60 mL) was heated under reflux (80–90 °C) under $N_2$ for 2 h. Hydrazine monohydrate (3.33 mL, 68.4 mmol) was added dropwise carefully and then refluxing of the mixture was continued for 48 h. After cooling, charcoal was added and the mixture was filtered. The solution was stirred at 0 °C to form a solid product, which was filtered off under suction. The crude product was dried under vacuum at 30 °C to give semitransparent white crystals (1.05 g, 42%), mp: 132 °C (DSC). FTIR (KBr, $cm^{-1}$): 3200–3400 (NH stretch). $^1$H NMR (500 MHz, DMSO-$d_6$, $\delta$, ppm): 6.57–7.12 (m, CH aromatic), 4.94 ($NH_2$), 1.57 [d, 6H, $C(CH_3)_2$]. $^{13}$C NMR (125 MHz, DMSO-$d_6$, $\delta$, ppm): 115.42–157.51 (aromatic), 30.83 [$C(CH_3)_2$].

**1,3,5-Tris(4-nitrophenoxy)benzene (Scheme S2†).** $K_2CO_3$ (40.0 g) was added to a solution of phloroglucinol (10.1 g, 0.0800 mol) in DMF (200 mL) and $H_2O$ (40 mL) under a $N_2$ atmosphere and then the mixture was heated under reflux (140 °C) for 6 h. After cooling to 70 °C, 4-fluoro-4-nitrobenzene (44.7 g, 0.310 mol) was added and then the mixture was again heated under reflux (150–160 °C) for 12 h under $N_2$. The mixture was cooled to room temperature and concentrated under reduced pressure; the residue was poured into 5% NaOH (500 mL) to afford a brown solid, which was filtered off, washed several times with distilled water, and dried under vacuum at 100 °C for 24 h. Recrystallization (pyridine/$H_2O$) afforded yellow crystals (9.56 g, 87%); mp (DSC): 200 °C. FTIR (KBr, $cm^{-1}$): 1584, 1341 ($NO_2$). $^1$H NMR (500 MHz, DMSO-$d_6$, $\delta$, ppm): 6.97–8.26 (m, aromatic). $^{13}$C NMR (125 MHz, DMSO-$d_6$, $\delta$, ppm): 109.57–162.56 (aromatic).

**1,3,5-Tris(4-aminophenoxy)benzene (Scheme S2†).** A mixture of 1,3,5-tris(4-nitrophenoxy)benzene (3.00 g, 6.14 mmol) and 10% Pd/C (0.300 g, 2.82 mmol) in anhydrous EA (50 mL) was stirred for 3 days under a $H_2$ atmosphere. The mixture was filtered and the filtrate concentrated under reduced pressure. The solid was extracted with $CH_2Cl_2$ (3 × 80 mL). The combined extracts were washed several times with distilled water, dried ($MgSO_4$, 30 min), and then concentrated under reduced pressure to give a white solid (2.00 g, 75%), mp: 90 °C (DSC). FTIR (KBr, $cm^{-1}$): 3200–3400 (NH stretch). $^1$H NMR (500 MHz, DMSO-$d_6$, $\delta$, ppm): 5.75–6.73 (m, CH aromatic), 4.97 (NH). $^{13}$C NMR (125 MHz, DMSO-$d_6$, $\delta$, ppm): 98.35–161.84 (aromatic).

**6-Methyl-3-phenyl-3,4-dihydrochromeno[6,7-*e*][1,3]oxazin-8(2*H*)-one (mono-coumarin BZ).** A solution of aniline (1.16 g, 12.5 mmol) and paraformaldehyde (0.716 g, 23.9 mmol) in 1,4-dioxane (100 mL) was stirred for 1 h in an ice bath and then a solution of coumarin–OH (2.00 g, 11.4 mmol) in 1,4-dioxane (50 mL) was added. The mixture was heated with stirring for 12 h under reflux. After cooling to room temperature, the solution was concentrated under reduced pressure to obtain a viscous oil, which was extracted into $CH_2Cl_2$ (3 × 100 mL). The combined extracts were washed several times with 1% $NaHCO_3$ and finally with distilled water, dried ($MgSO_4$, 1 h), and concentrated under reduced pressure to give a yellow solid, which was purified through column chromatography ($SiO_2$; *n*-hexane/EA, 1 : 1) to obtain a white solid (1.3 g, 65%); mp (DSC): 142 °C. FTIR (KBr, $cm^{-1}$): 1263 (asymmetric COC stretching), 1341 ($CH_2$ wagging), 937 and 1490 (vibrations of trisubstituted benzene ring), 1733 (C=O stretching). $^1$H NMR (500 MHz, DMSO-$d_6$, $\delta$, ppm): 6.79–7.54 (m, CH aromatic), 6.21 (s, 1H, CH), 5.55 (s, 2H, $OCH_2N$), 4.75 (s, 2H, $CCH_2N$), 2.36 (s, 3H, $CCH_3$). $^{13}$C NMR (125 MHz, DMSO-$d_6$, $\delta$, ppm): 108.96–157.89 (aromatic), 160.60 (C=O), 79.81 ($OCH_2N$), 44.85 ($CCH_2N$), 18.22 ($CH_3$). High resolution FT-MS $[M]^+$ *m*/*z* for $C_{18}H_{16}NO_3$: 294.12: calcd: 294 (Fig. S1†).

**4-Dihydrochromeno[6,7-*e*][1,3]oxazin-8(2*H*)-one (di-coumarin BZ) (Scheme S1†).** A solution of bisphenol A–$NH_2$ (0.800 g, 1.95 mmol), coumarin–OH (0.721, 4.10 mmol), and paraformaldehyde (0.246 g, 8.19 mmol) in 1,4-dioxane (70 mL) was heated under reflux (90–100 °C) with stirring under $N_2$. After 24 h, the solution was cooled to room temperature and concentrated under reduced pressure. The solid residue was extracted into $CH_2Cl_2$ (3 × 100 mL); the combined extracts were washed several times with 1 N NaOH and then with distilled water, dried ($MgSO_4$, 40 min), and then concentrated under pressure to obtain a yellow solid (1.00 g, 57%). FTIR (KBr, $cm^{-1}$): 1727 (C=O stretch), 1383 ($CH_2$ wagging), 1239 (asymmetric COC stretching), 1059 (symmetric C–O–C stretching), 932 (vibration of trisubstituted benzene ring) (Fig. S1†). $^1$H NMR (500 MHz, DMSO-$d_6$, $\delta$, ppm): 6.77–7.53 (m, CH aromatic), 6.20 (d, 1H, CCH), 5.50 (s, 2H, $OCH_2N$), 4.70 (s, 2H, $CCH_2N$), 2.35 (d, 3H, $CH_3$), 1.55 [d, 6H, $C(CH_3)_2$]. $^{13}$C NMR (125 MHz, DMSO-$d_6$, $\delta$, ppm): 160.58 (C=O), 108.83–157.85 (aromatic carbon resonances), 80.25 ($OCH_2N$), 45.29 ($CCH_2N$), 30.74 ($C(CH_3)_2$), 18.21 ($CH_3$). High resolution FT-MS $[M]^+$ *m*/*z* for $C_{51}H_{43}N_2O_8$: 811.30: calcd: 811.10 (Fig. S3†).

**3,3′,3″-(4,4′,4″-(Benzene-1,3,5-triyltris(oxy))tris(benzene-4,1-diyl))tris(6-methyl-3,4-dihydrochromeno[6,7-*e*][1,3]oxazin-8(2*H*)-one) (tri-coumarin BZ) (Scheme S2†).** A solution of 1,3,5-tris(4-aminophenoxy)benzene (1.50 g, 3.76 mmol), coumarin–OH (2.12 g, 12.0 mmol), and paraformaldehyde (0.688 g, 22.9 mmol) in 1,4-dioxane (60 mL) was heated under reflux (80–90 °C) with stirring under $N_2$. The reaction was monitored using thin layer chromatography (TLC). After 48 h, the solution was cooled to room temperature and filtered. The filtrate was concentrated under reduced pressure to obtain a yellow solid, which was extracted into $CH_2Cl_2$ (3 × 100 mL); the combined extracts were washed several times with 1 N NaOH, dried

Published on 21 January 2016. Downloaded by Universitaet Osnabrueck on 29/01/2016 03:31:33.

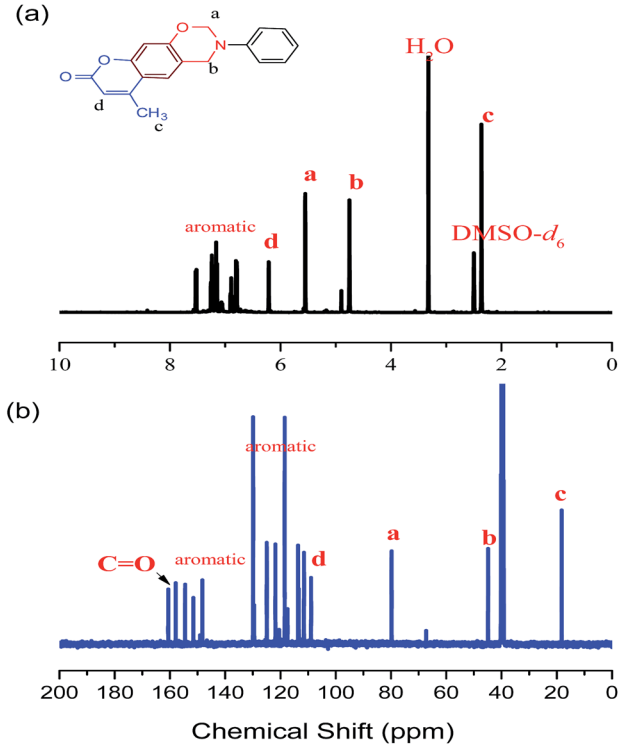


Fig. 1 (a) $^{1}$H and (b) $^{13}$C NMR spectra of mono-coumarin BZ.

(MgSO$_4$, 1 h), and concentrated under reduced pressure to obtain a yellow solid (0.50 g, 34%); FTIR (KBr, cm$^{-1}$): 1383 ($CH_2$ wagging), 1260 (asymmetric COC stretching), 1059 (C–O–C stretching), 932 (vibration of trisubstituted benzene ring), 1727 (C═O stretch) (Fig. S2†). $^{1}$H NMR (500 MHz, DMSO-$d_6$, $\delta$, ppm): 6.79–7.53 (aromatic), 6.20 (t, 1H, CCH), 5.48 (t, 2H, $OCH_2N$), 4.70 (t, 2H, $CCH_2N$), 2.35 (t, 3H, $CH_3$). $^{13}$C NMR (125 MHz, DMSO-$d_6$, $\delta$, ppm): 160.56 (C═O), 101.07–157.83 (aromatic), 80.10 ($OCH_2N$), 45.13 ($CCH_2N$), 18.20 ($CCH_3$). High resolution FT-MS $[M]^+$ $m/z$ for $C_{60}H_{46}N_3O_{12}$: 1000.31: calcd: 1000.00 (Fig. S5†).

### Thermal curing of mono-, di-, and tri-coumarin BZ

Desired amounts of (mono, di-and tri-coumarin BZ) were put onto aluminum pans and polymerized in stepwise manner: at 150 °C, 180 °C, 210 °C, and 240 °C for 2 h. Each thermal curing sample has the red color and more dark as curing temperature increasing. After completing the curing process, samples were cooled to room temperature. The same procedures were done with (mono, di-and tri-coumarin BZ) after photo-dimerization of coumarin unit.

### Photo-dimerization of coumarin-functionalized benzoxazine (Scheme 2)

An appropriate amount of coumarin BZ (0.1 g) was dissolved in dichloromethane (20 mL) was placed in quartz tube. The tube

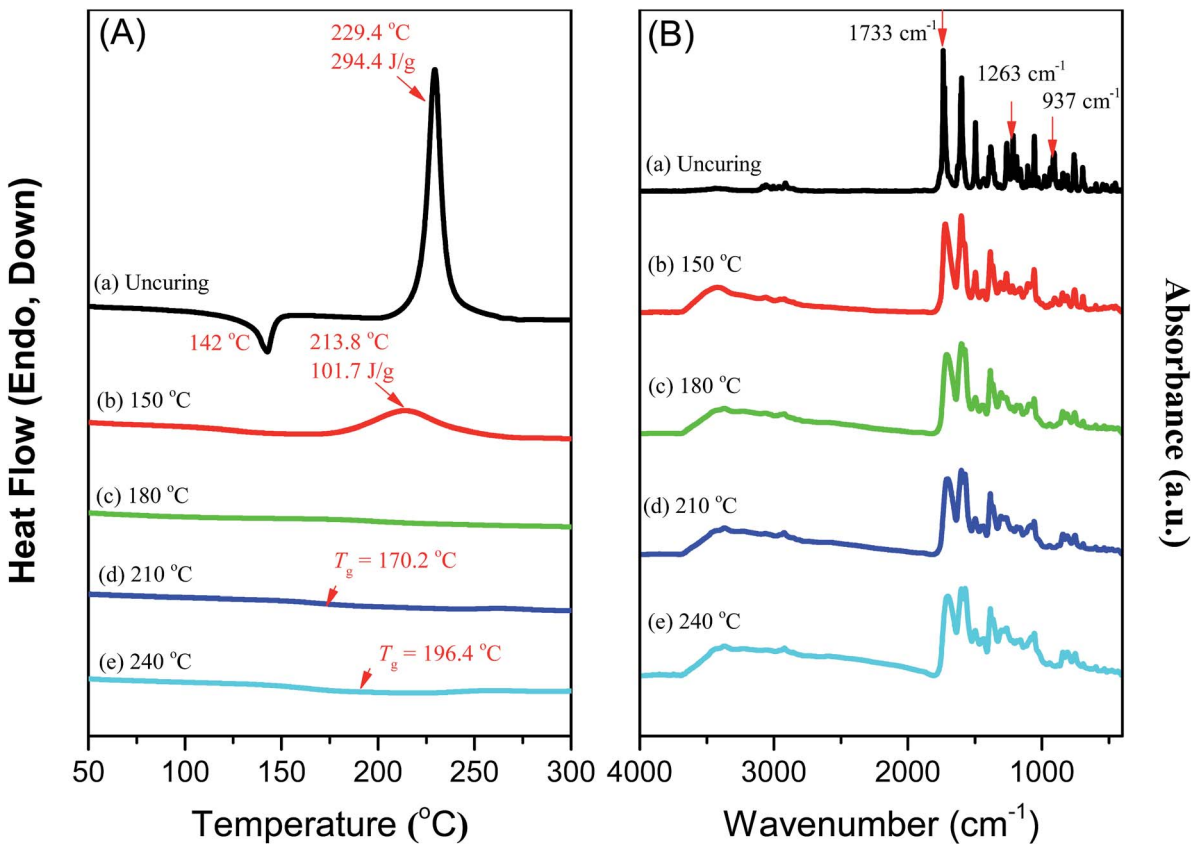


Fig. 2 (A) DSC thermograms and (B) FTIR spectra of mono-coumarin BZ, recorded after each curing stage.


This journal is © The Royal Society of Chemistry 2016

Published on 21 January 2016. Downloaded by Universitaet Osnabrueck on 29/01/2016 03:31:33.

was irradiated in the Carousel equipped with 15 Philips lamps emitting light nominally at 365 nm for 50 min at room temperature.

### Samples of coumarin-functionalized benzoxazines for contact angle measurements

A solution of coumarin Bz (0.06 g) was dissolved in 2 mL of dichloromethane (DCM), filtered at room temperature through a 0.2 μm syringe filter before and after UV exposure and then spin-coated onto a glass substrate with rotating speeds 1100 rpm for 15 s. The samples were thermally polymerized in an oven at 150, 180, 210, and 240 °C for 2 h for each step.

### Characterization

$^1$H and $^{13}$C NMR spectra were recorded using an INOVA 500 instrument with DMSO-$d_6$ and $CDCl_3$ as solvents. FTIR spectra were recorded using a Bruker Tensor 27 spectrophotometer and the conventional KBr disk method, with 32 scans at a spectral resolution of 4 cm$^{-1}$. The polymer films were sufficiently thin to obey the Beer–Lambert law. Elevated-temperature FTIR spectra were recorded in the temperature-controlled compartment of the spectrometer. The molecular weights of (mono-, di-, and tri-coumarin BZ), were recorded using a Bruker Solarix high resolution Fourier Transform Mass spectroscopy system FT-MS (Bruker, Bremen, Germany). Dynamic curing kinetics and glass transition temperatures were measured using a TA Q-20 DSC apparatus operated under a $N_2$ atmosphere. The sample (*ca.* 5–10 mg) was placed in a sealed aluminum sample pan. The dynamic thermal curing behavior was recorded during the first heating scan from 30 to 350 °C at a heating rate of 20 °C min$^{-1}$; the glass transition temperature behavior was recorded during the second heating scan from −90 to 350 °C at a heating rate of 20 °C min$^{-1}$ from the sample quenched at 300 °C. The thermal decomposition and char yield of PBZs were determined using a TA Q-50 TGA analyzer operated under a $N_2$ atmosphere. The uncured and cured PBZs samples (*ca.* 5–10 mg) were placed in a Pt cell and heated from 30 to 800 °C under a $N_2$ atmosphere at a heating rate of 20 °C min$^{-1}$. Photo-dimerization of coumarin units was performed directly under a UV-Vis lamp at 365 nm (power: 90 mW cm$^{-1}$); corresponding UV-Vis spectra were recorded by using a Shimadzu mini 1240 spectrophotometer. Water contact angles were measured using an FDSA Magic Droplet 100 contact angle goniometer interfaced with image capture software; droplets (5 μL) of deionized water at room temperature were placed on the PBZs samples before and after photo-dimerization of the coumarin units.

## Results and discussion

### Preparation for three different functionalities of coumarin moieties functionalized benzoxazine monomers

In this study, we synthesized benzoxazine monomers presenting one, two, and three coumarin units, respectively. We suspected that, after thermal curing of these benzoxazine monomers, photodimerization, through [2π + 2π] cycloaddition, of the coumarin units in the PBZs would enhance their glass transition temperatures ($T_g$), degradation temperatures ($T_d$), char yields, and hydrophobic surface properties. In a previous study, we synthesized 4-methyl-7-hydroxycoumarin (coumarin–OH) through an acid-catalyzed reaction of resorcinol and ethyl acetoacetate.[31] Here, we used coumarin–OH as a common phenolic heterocyclic material to prepare our three different coumarin-containing monomers to provide PBZs as photoresponsive crosslinking materials (Scheme 1).

We synthesized 6-methyl-3-phenyl-3,4-dihydrochromeno [6,7-*e*][1,3]oxazin-8(2*H*)-one (mono-coumarin BZ) through the reaction of paraformaldehyde, aniline, and coumarin–OH in 1,4-dioxane. We synthesized 4-dihydrochromeno[6,7-*e*][1,3]oxazin-8(2*H*)-one (di-coumarin BZ) in two steps (Scheme 1 and Fig. S2†): reduction of 2,2-bis(4-(4-nitrophenoxy)-phenyl) propane (bisphenol–$NO_2$) over Pd/C in hydrazine monohydrate afforded bisphenol A–$NH_2$; subsequent reaction of bisphenol–$NH_2$, coumarin–OH, and paraformaldehyde in 1,4-dioxane provided di-coumarin BZ. We synthesized tri-coumarin BZ in high purity in three steps (Scheme 1 and Fig. S4†): the reaction of phloroglucinol with 1-fluoro-4-nitrobenzene in the presence of $K_2CO_3$ in DMF produced 1,3,5-tris(4-nitrophenoxy) benzene, which we reduced over Pd/C under $H_2$ at ambient temperature to afford 1,3,5-tris(4-aminophenoxy)benzene,

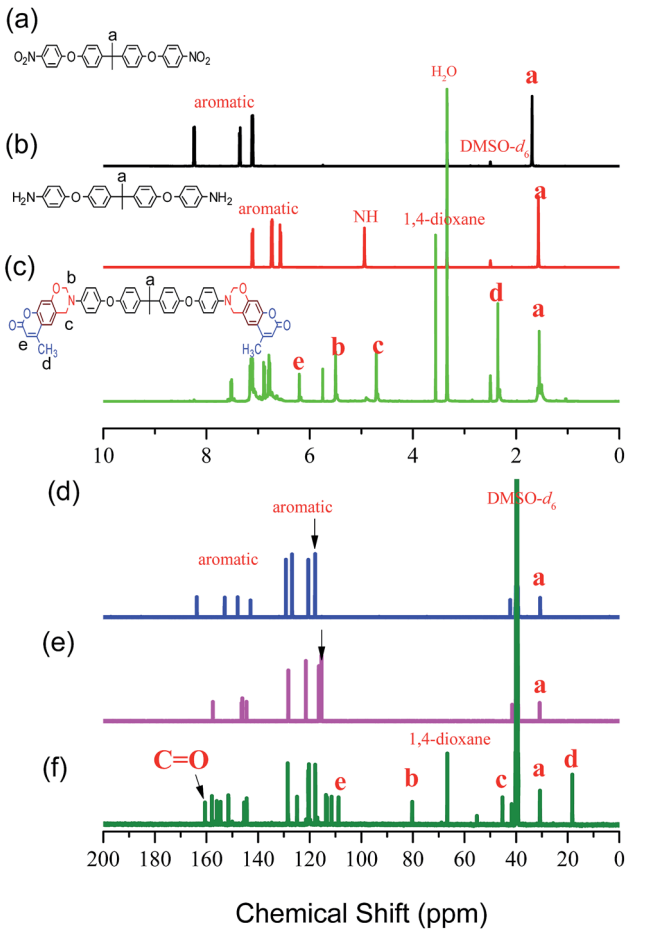


Fig. 3 (a–c) $^1$H and (d–f) $^{13}$C NMR of (a and d) bisphenol A–$NO_2$, (b and e) bisphenol A–$NH_2$, and (c and f) di-coumarin BZ.

Published on 21 January 2016. Downloaded by Universitaet Osnabrueck on 29/01/2016 03:31:33.

which we reacted with coumarin–OH and paraformaldehyde through the Mannich reaction in 1,4-dioxane to afford tri-coumarin BZ.

### Characterization of mono-coumarin BZ

We used FTIR and NMR spectroscopy to confirm the chemical structures of our coumarin-functionalized benzoxazines. Fig. 1(a) presents the $^1$H NMR spectrum of mono-coumarin-BZ in *d*-DMSO. The signals ranging from 6.22 to 7.54 ppm represent the aromatic protons; the peaks at 6.20 and 2.36 ppm correspond to the CH=C and $CH_3$ groups of the coumarin unit. The benzoxazine ring of mono-coumarin BZ is characterized by signals at 4.75 (Ar**C**$\mathbf{H}_2$N) and 5.55 (O**C**$\mathbf{H}_2$N) ppm; the relative intensity of these two signals is 1 : 1, confirming the high purity of this benzoxazine monomer. Fig. 1(b) displays the corresponding $^{13}$C NMR spectrum, with signals at 159.76 and 18.13 ppm for the **C**=O and **C**$H_3$ groups of the coumarin unit and characteristic signals for the Ar**C**$H_2$N and O**C**$H_2$N groups of the benzoxazine ring at 44.61 and 79.38 ppm, respectively. These spectra confirmed the chemical structure of mono-coumarin BZ.

We employed DSC and FTIR spectroscopy to investigate the thermal polymerization behavior of mono-coumarin BZ (Fig. 2). The melting point of the uncured mono-coumarin BZ monomer was 142 °C, confirming its high purity, with a curing exotherm peak centered at 229.4 °C and a reaction heat of 294.4 J g$^{-1}$ [Fig. 2(A)-(a)]. The curing exotherm temperature of mono-coumarin BZ was much lower than that of the model compound 3-phenyl-3,4-dihydro-2*H*-benzooxazine (Pa) (263 °C) lacking the coumarin unit; its curing peak appeared at 263.0 °C, implying that the coumarin unit acted as a catalyst that lowered the curing temperature and a strong electron withdrawing electron conjugated C=C bond in coumarin unit.[30,31] After thermal curing at 150 °C, the melting point disappeared and the curing exotherm peak and the reaction heat decreased to 213.8 °C and 101.7 J g$^{-1}$, respectively. The curing exotherm peak disappeared completely after thermal curing at 180 °C; glass transition temperatures of 170.2 and 196.4 °C appeared after thermal curing at 210 and 240 °C, respectively. FTIR spectra revealed the main characteristic absorption peaks of the uncured mono-coumarin BZ monomer at 937 cm$^{-1}$ (out-of plane C–H bending) and 1263 cm$^{-1}$ (C–O–C stretching);[32–37] both of these signals decreased gradually upon increasing the curing polymerization temperature, disappearing almost completely after curing at 240 °C.

### Characterization of di-coumarin BZ

Fig. 3 presents the NMR spectra of bisphenol A–$NO_2$, bisphenol A–$NH_2$, and di-coumarin BZ in *d*-DMSO. The $^1$H NMR spectrum of bisphenol A–$NO_2$ [Fig. 3(a)] features signals at 7.10–8.25 ppm for the aromatic protons and 1.57 ppm for the C(C$\mathbf{H}_3$)$_2$ protons; a signal at 4.95 ppm appears in Fig. 3(b) for the N**H** proton of bisphenol A–$NH_2$. The $^1$H NMR spectrum [Fig. 3(c)] of di-coumarin-BZ features signals in the range from 6.73 to 7.54 ppm corresponding to the aromatic protons, and signals at 6.17 and 2.34 ppm for CH=C and $CH_3$ groups, respectively, of

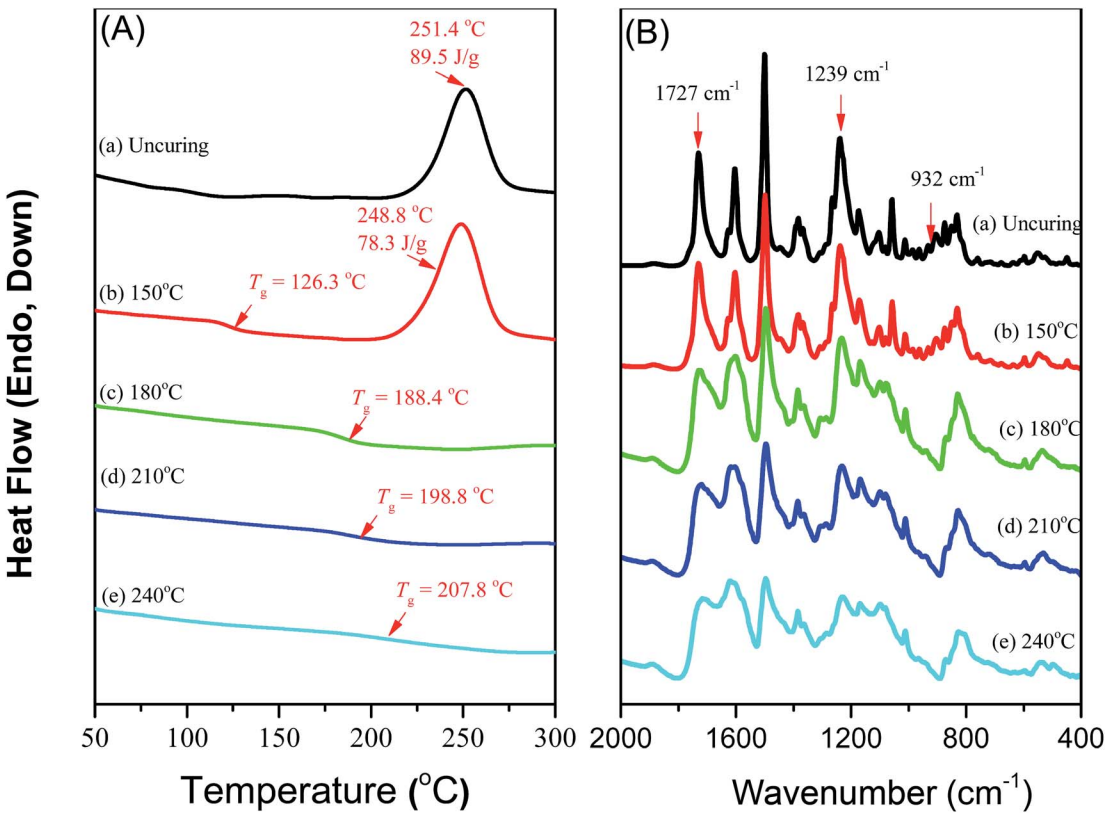


Fig. 4 (A) DSC thermograms and (B) FTIR spectra of di-coumarin BZ, recorded after each curing stage.

 This journal is © The Royal Society of Chemistry 2016

Published on 21 January 2016. Downloaded by Universitaet Osnabrueck on 29/01/2016 03:31:33.

the coumarin unit. Characteristic signals of the benzoxazine ring appear at 4.71 and 5.50 ppm for the Ar**C**$H_2$N and O**C**$H_2$N groups, respectively. Moreover, the integration area of the two proton signals Ar$CH_2$N and O$CH_2$N was close to 1 : 1; confirming the high purity of this benzoxazine monomer. Fig. 3(d)–(f) present the $^{13}$C NMR spectra of bisphenol A–$NO_2$, bisphenol A–$NH_2$, and di-coumarin-BZ. The successful reduction of bisphenol A–$NO_2$ to bisphenol A–$NH_2$ was characterized by the disappearance of the signal at 120.0 ppm [Fig. 3(d)] for the Ar**C**$NO_2$ group and the appearance of a signal at 117.3 ppm for the Ar**C**$NH_2$ group [Fig. 3(e)]. We observed characteristic signals at 160 (**C**=O), 79.8 (O$CH_2$N), 45.1 (Ar$CH_2$N), and 18.1 (**C**$H_3$) ppm for di-coumarin BZ [Fig. 3(f)], confirming the successful introduction the coumarin units into the benzoxazine rings.

Again, we employed DSC to monitor the behavior of di-coumarin BZ before and after thermal curing at 150, 180, 210, and 240 °C. Fig. 4(A) presents the DSC analyses for this monomer recorded at a heating rate of 20 °C min$^{-1}$. An exothermic peak for di-coumarin BZ was centered at 251.4 °C, with a reaction heat of 89.5 J g$^{-1}$. We observed two interesting phenomena for this system: (a) a glass transition temperature was evident for all curing temperatures, with the value of $T_g$ increasing, from 126.3 to 207.8 °C, upon increasing the thermal curing temperature; (b) the glass transition temperature (207.8 °C) of poly(di-coumarin BZ) was higher than that of poly(mono-coumarin BZ) (196.4 °C) after thermal curing at 240 °C, consistent with a higher crosslinking density for poly(di-coumarin BZ). Fig. 4(B) presents corresponding FTIR spectra of di-coumarin BZ recorded before and after thermal curing. Characteristic absorption peaks of the benzoxazine ring structure of the monomer, for C–O–C and C–N–C stretching and the benzene ring mode appeared at 1239, 1186, and 932 cm$^{-1}$, respectively. After thermal curing at 180, 210, and 240 °C, the characteristic absorption peak at 932 cm$^{-1}$ (out-of plane C–H bending) disappeared from the spectrum of poly(di-coumarin BZ), with the signal of the C=O groups at 1733 cm$^{-1}$ shifting to lower wavenumber, due to hydrogen bonding between the C=O groups of the coumarin units and phenolic OH groups.

## Characterization of tri-coumarin BZ

Fig. 5 displays NMR spectra of 1,3,5-tris(4-nitrophenoxy) benzene, 1,3,5-tris(4-aminophenoxy)benzene, and tri-coumarin BZ. Three signals appeared for the aromatic protons of 1,3,5-tris(4-nitrophenoxy)benzene at 6.94, 7.30, and 8.28 ppm [Fig. 5(a)]; a signal at 4.90 ppm corresponding to the NH protons and signals at 5.91–6.74 ppm for the aromatic protons were present in the spectrum of 1,3,5-tris(4-aminophenoxy)benzene [Fig. 5(b)]. The $^1$H NMR spectrum of tri-coumarin-BZ [Fig. 5(c)] features signals at 6.17 and 2.34 ppm corresponding to the C**H**=C and C**H**$_3$ groups of the coumarin units, with characteristic signals for the benzoxazine ring at 4.70 and 5.55 ppm (Ar**C**$H_2$N and O**C**$H_2$N groups, respectively). The $^{13}$C NMR spectrum of tri-coumarin BZ [Fig. 5(f)] confirmed its chemical structure, with signals at 79.88 and 45.05 ppm corresponding to the characteristic resonances of the O$CH_2$N and Ar$CH_2$N groups, respectively, in the oxazine ring, and

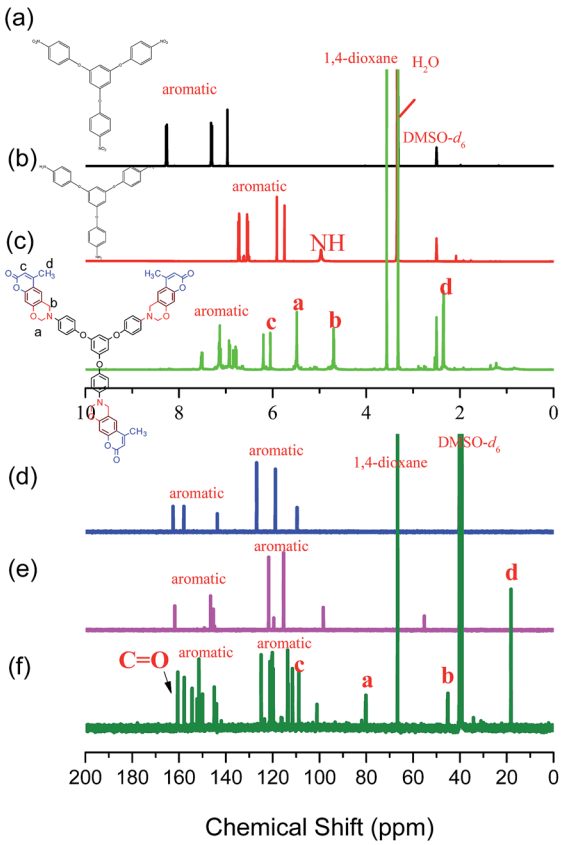


Fig. 5 (a–c) $^1$H and (d–f) $^{13}$C NMR of (a and d) 1,3,5-tris(4-nitophenoxy)benzene, (b and e) 1,3,5-tris(4-aminophenoxy)benzene, and (c and f) tri-coumarin BZ.

signals at 160 and 18.1 ppm representing the C=O and C$H_3$ groups, respectively, of the coumarin units.

We used DSC and FTIR spectroscopy to study the thermal curing polymerization of tri-coumarin BZ. The DSC thermogram of uncured tri-coumarin BZ features a sharp exothermic peak centered at 241.4 °C, with a reaction heat of 146.1 J g$^{-1}$ [Fig. 6(A)]. The reaction heat of the exotherm peak decreased gradually upon increasing the curing temperature, disappearing completely after thermal curing at 240 °C. Compared with the behavior of mono-coumarin-BZ and di-coumarin-BZ, the curing peak shifted to higher temperature upon increasing the temperature because the relatively higher crosslinking density of tri-coumarin-BZ inhibited its thermal curing ability, with complete thermal curing occurring only at 240 °C, much higher than the complete thermal curing temperatures of mono-coumarin BZ and di-coumarin BZ (180 °C). Because of the relatively higher crosslinking density arising from the greater number of aromatic heterocyclic groups in poly(tri-coumarin BZ), its glass transition temperature (240.5 °C) was higher than those of poly(mono-coumarin BZ) (196.4 °C) and poly(di-coumarin BZ) (207.8 °C). Fig. 6(B) presents FTIR spectra of tri-coumarin BZ before and after thermal curing, revealing phenomena similar to those for mono-coumarin BZ and di-coumarin BZ. After thermal curing at 240 °C, the characteristic absorption signals for the monomer at 1502, 1379, 1238 and 932

Published on 21 January 2016. Downloaded by Universitaet Osnabrueck on 29/01/2016 03:31:33.

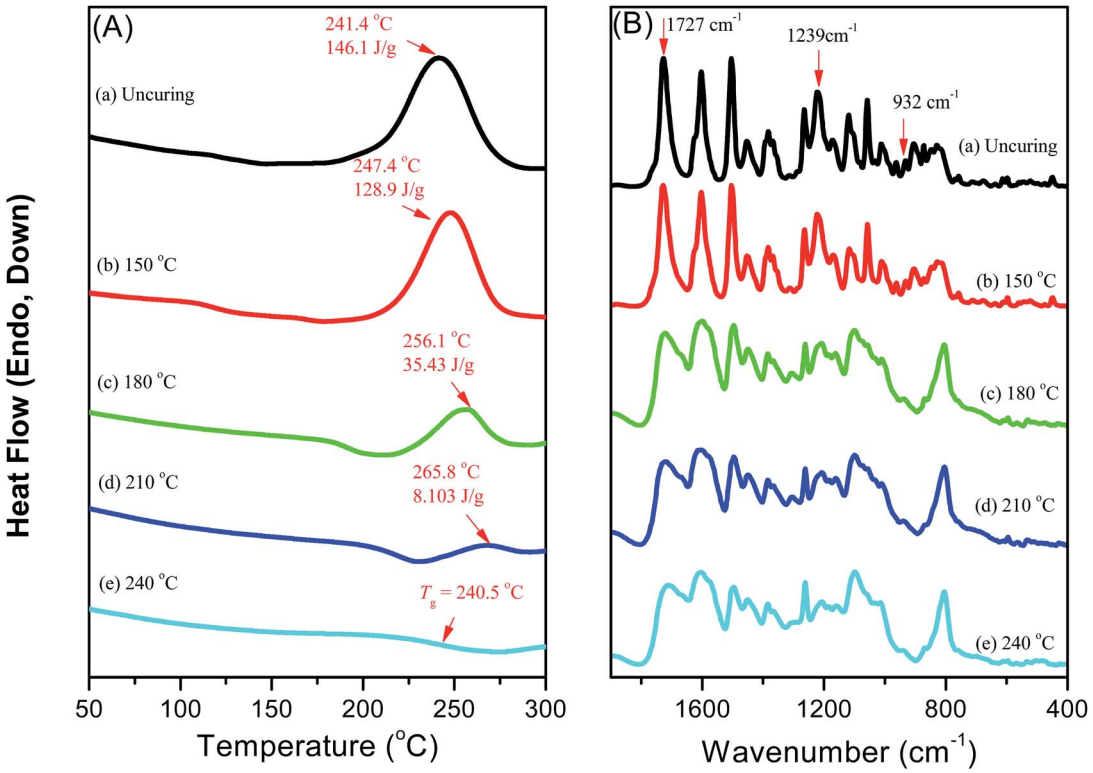


Fig. 6 (A) DSC thermograms and (B) FTIR spectra of tri-coumarin BZ, recorded after each curing stage.

$cm^{-1}$ disappeared from the spectrum of poly(tri-coumarin BZ), indicating that completely ring opening of benzoxazine ring.

### TGA of mono-, di-, and tri-coumarin BZ

Fig. 7 presents TGA thermograms of the mono-, di-, and tri-coumarin BZ monomers before and after thermal curing at 150, 180, 210, and 240 °C at a heating rate 20 °C $min^{-1}$ under $N_2$. We observed two phenomena. First, the thermal decomposition temperature and char yield both increased upon increasing the thermal curing temperature for each of these three coumarin-functionalized BZ monomers. We attribute the weight loss for these three different monomers to amine evaporation through Mannich base cleavage and phenol and coumarin degradation.[30] Second, the thermal decomposition temperature and char yield of poly(tri-coumarin BZ) were higher (370 °C and 52.43 wt%, respectively) than those of poly(mono-coumarin BZ) (336 °C and 51.39 wt%, respectively) and poly(di-coumarin BZ) (366 °C and 46.29 wt%, respectively), due to it having the network with the highest crosslinking density.[30,31] In addition, we also examined the thermal stability of the model poly(Pa BZ) lacking the coumarin unit; its char yield was 43 wt%. Thus, the thermal stabilities our three coumarin-functionalized BZ derivatives were better than that of the Pa-type benzoxazine after thermal curing.

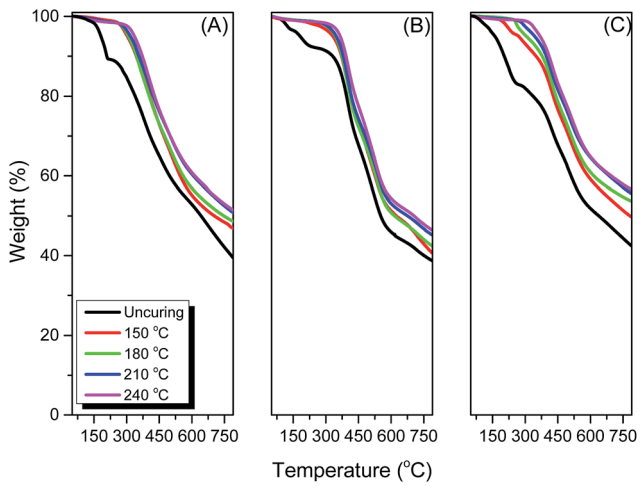


Fig. 7 TGA analyses of (A) mono-coumarin BZ, (B) di-coumarin BZ, and (C) tri-coumarin BZ, recorded after each curing stage.

### Photodimerization through [2π + 2π] cycloaddition of coumarin moieties

Coumarin units can undergo photochemical dimerization through [2π + 2π] cycloaddition in direct and sensitized reactions *via* singlet and triplet excited states.[38,39] Fig. 8(A) displays the UV-Vis spectrum of mono-coumarin BZ after photodimerization [Scheme 2(a)] of its coumarin unit under UV irradiation (350 nm) at a concentration of $10^{-4}$ M. The typical absorption peaks of coumarin and its derivatives appear between 250 and 300 nm, corresponding to π–π* transitions, with another π–π* absorption signal, due to the pyrone unit, appearing between 310 and 340 nm.[28c,31a,40,41] As revealed in Fig. 8(A), UV irradiation for 30 min led to a decrease in the

 This journal is © The Royal Society of Chemistry 2016

Published on 21 January 2016. Downloaded by Universitaet Osnabrueck on 29/01/2016 03:31:33.

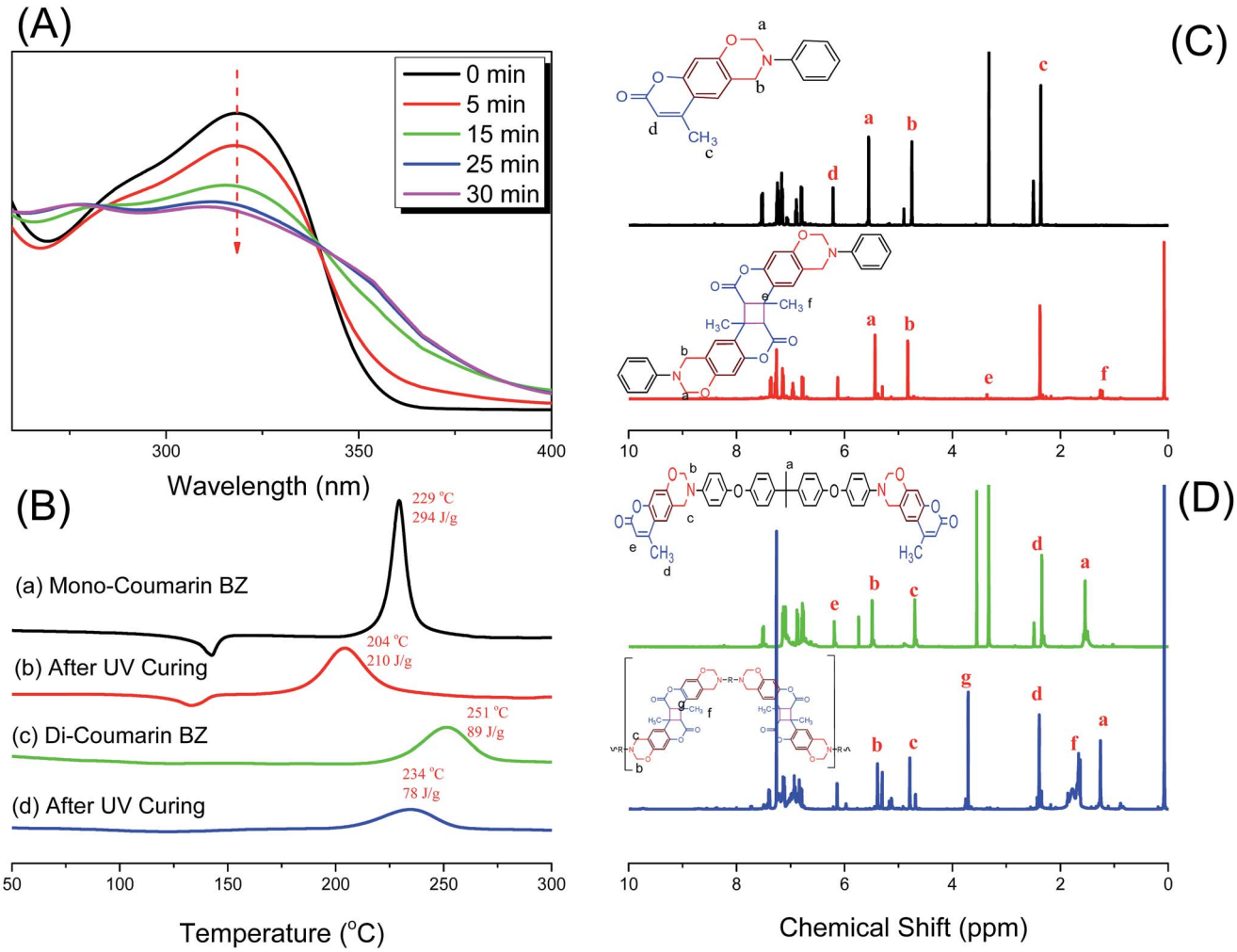


Fig. 8 (A) Changes in UV-Vis absorbance of mono-coumarin BZ solutions in THF after irradiation at 365 nm. (B) DSC traces of mono- and di-coumarin BZ before and after photodimerization of their coumarin units. (C and D) $^1$H NMR spectra of (C) mono-coumarin BZ and (D) di-coumarin BZ before and after photodimerization.

intensity of the absorption signal at 318 nm, confirming that dimerization through [2π + 2π] cycloaddition of the olefinic bond destroyed the delocalized π system. We calculated the degree of photodimerization of the 4-methylcoumarin moieties of mono-coumarin BZ using the equation[28c,31a]

$$\text{Photodimerization degree} = (1 - A_t/A_0) \times 100\%$$

where $A_0$ and $A_t$ are the absorbance of the coumarin unit at 318 nm initially and after irradiation for time $t$, respectively. After irradiation for 30 min, the degree of dimerization for this system was approximately 35%. Fig. 8(B) and S6–S8† present DSC thermograms of mono-, di-, and tri-coumarin BZ before and after [2π + 2π] dimerization of their coumarin moieties. As mentioned above in our discussion of Fig. 2(A) and 3(A), the exothermic peaks of mono-coumarin BZ and di-coumarin BZ appeared at 229 and 251 °C, respectively. The curing exotherm peak shifted to lower temperature and the reaction heat decreased (for mono-coumarin BZ: $T_p$, 204 °C; $\Delta H$, 210 J g$^{-1}$; for di-coumarin BZ: $T_p$, 234 °C; $\Delta H$, 78 J g$^{-1}$) after photodimerization of each monomer, due to destruction of the benzoxazine surface units during irradiation.[30,31] Yagci *et al.* reported that various isomers, with different *syn*, *anti*, head-to-head, and head-to-tail configurations for the $CH_3$ groups, can form after UV irradiation.[30] Fig. 8(C) and (D) displays $^1$H NMR spectra of mono- and di-coumarin BZ before and after UV irradiation for 30 min in $CDCl_3$. After their photodimerization, as presented in Schemes 2(a) and (b), two new characteristic signals appeared at 3.7 and 1.4 ppm, representing the protons of the C**H** group (peak e) of the cyclobutane and the C**H**$_3$ group (peak f), respectively. In addition, the intensity of the signal at 6.20 ppm for the C**H**═C group of the coumarin unit decreased to approximately 35% [Fig. 8(C)], consistent with the behavior observed in the UV-Vis spectrum [Fig. 8(A)]. Thus, the $^1$H NMR spectra provided strong evidence for dimerization of the coumarin moieties in these coumarin-functionalized BZ monomers. Fig. 9 displays TGA traces (under $N_2$) of the uncured di-coumarin BZ, the poly(di-coumarin BZ) obtained after thermal curing alone, and the poly(di-coumarin BZ) obtained after both photodimerization and thermal curing. Here, we

Published on 21 January 2016. Downloaded by Universitaet Osnabrueck on 29/01/2016 03:31:33.

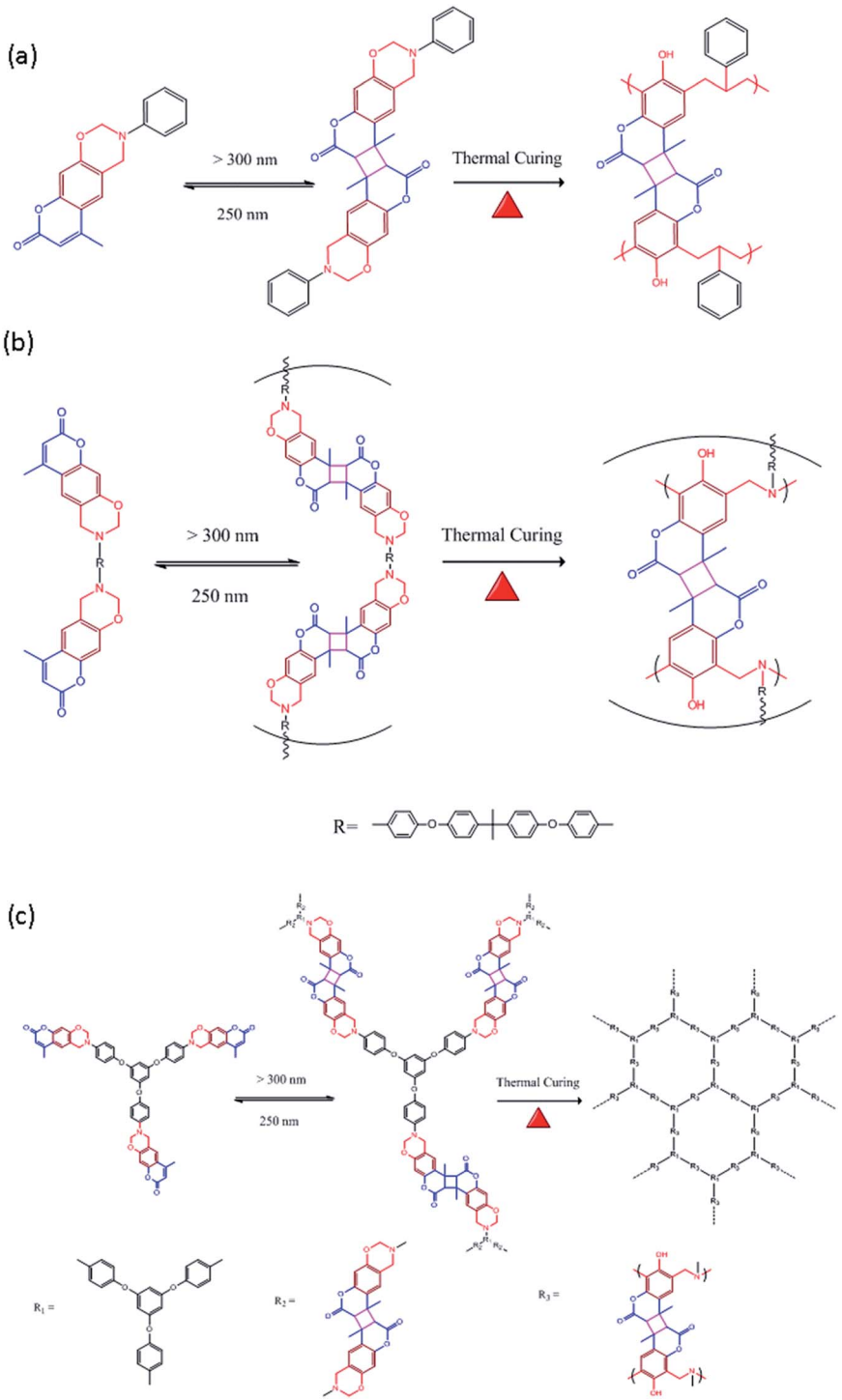


Scheme 2 Photodimerization of (a) mono-coumarin BZ, (b) di-coumarin BZ, and (c) tri-coumarin BZ, with subsequent thermal curing to form PBZ matrices of high crosslinking density.

used the 10 wt% weight loss temperature ($T_d$) 321, 381, 398, and 365 °C, respectively-as a proxy for the thermal stability. The value of $T_d$ of poly(di-coumarin BZ) gradually increased upon increasing the curing temperature, with a char yield of 46 wt% after thermal curing at 240 °C. Interestingly, both photodimerization and thermal curing gave a poly(di-coumarin BZ) displaying a degradation temperature that decreased, possibly as a result of destruction of the surface during irradiation, whereas the char yield increased slightly to 48 wt% because of the relatively higher crosslinking density after UV irridation.[31] We employed DSC to monitor the effect of photo-crosslinking of the coumarin units under UV irradiation (300 nm) on the glass transition temperatures of the PBZ matrices formed from our three different coumarin-functionalized PBZs (Fig. 10). The

 This journal is © The Royal Society of Chemistry 2016

Published on 21 January 2016. Downloaded by Universitaet Osnabrueck on 29/01/2016 03:31:33.

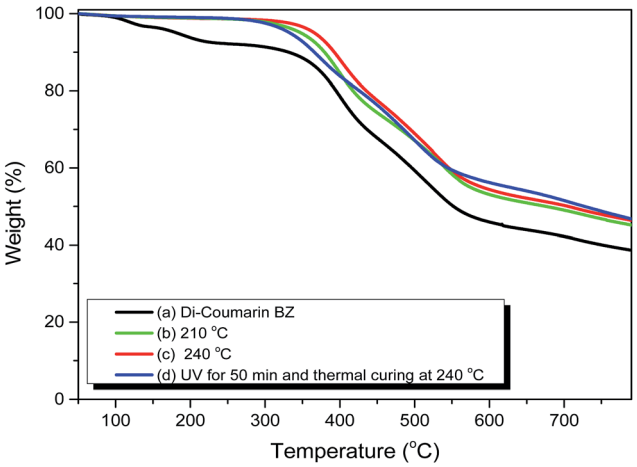


Fig. 9 TGA analyses of di-coumarin BZ: (a) uncured monomer; (b and c) after thermal curing at (b) 210 and (c) 240 °C, and after both photodimerization and thermal curing at 240 °C.

glass transition temperature increased for each of our coumarin-functionalized benzoxazine monomers after photodimerization. For example, the values of $T_g$ increased from 170.0 to 203.4 °C, from 198.8 to 210.1 °C, and from 218.8 to 260.0 °C for poly(mono-coumarin BZ), poly(di-coumarin BZ), and poly(tri-coumarin BZ), respectively, after combining photodimerization with thermal curing at 210 °C. We attribute these increases in glass transition temperature to the increased crosslinking density of the PBZs after photodimerization of their coumarin units. The polymer formed from the trivalent coumarin/benzoxazine displayed the highest glass transition and thermal decomposition temperatures and char yield, as would be expected from the highest crosslinking density for this compound, the presence of methyl group in the repeating unit and the additional crosslinking reaction through the transesterification of COO group in coumarin unit and OH groups which generated after ring opening thermal polymerization of benzoxazine as displayed in Scheme 2(c).[31b]

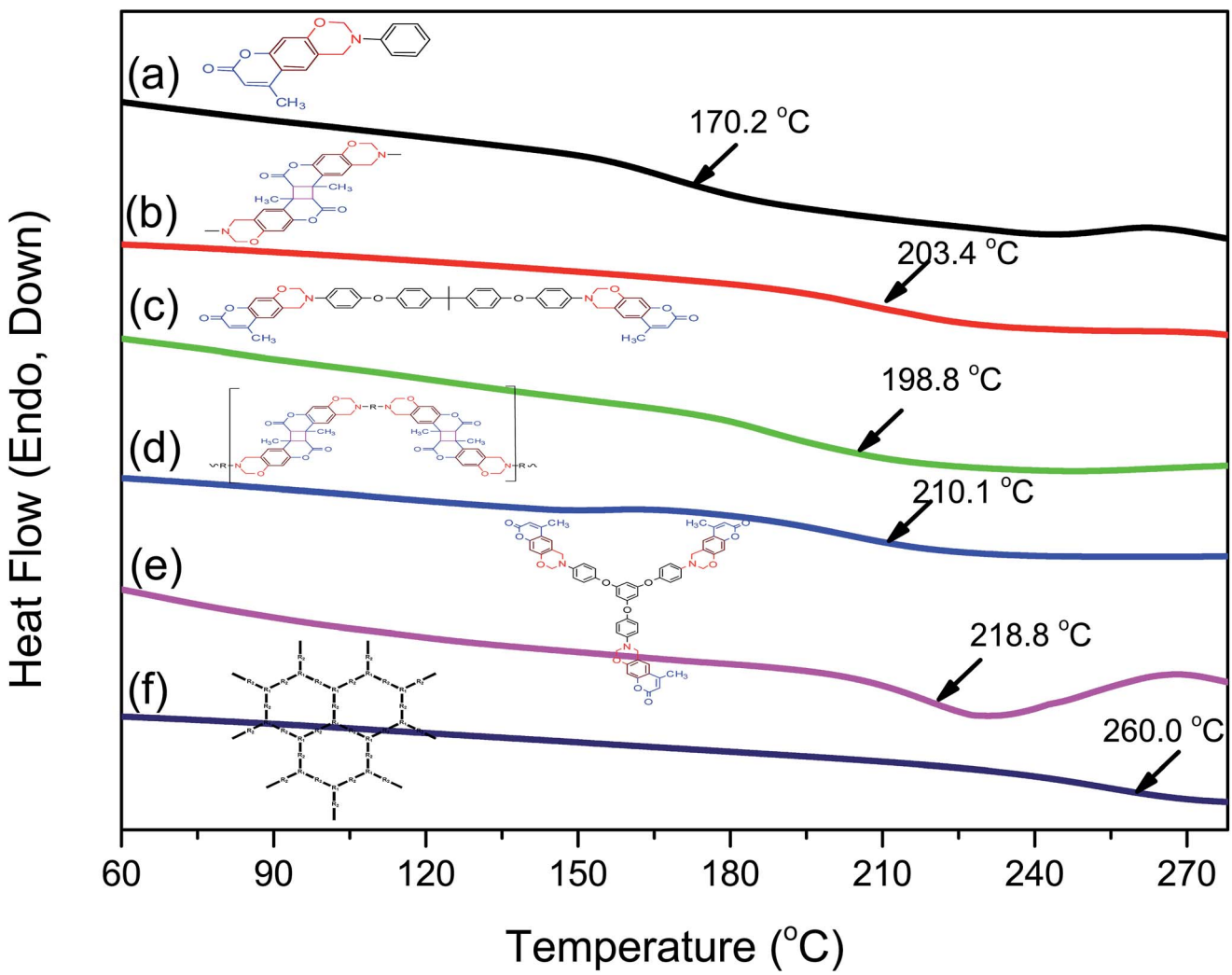


Fig. 10 DSC analyses of (a and b) poly(mono-coumarin BZ), (c and d) poly(di-coumarin BZ), and (e and f) poly(tri-coumarin BZ) after (a, c and e) thermal curing at 210 °C and (b, d and f) sequential photodimerization and thermal curing at 210 °C.

Published on 21 January 2016. Downloaded by Universitaet Osnabrueck on 29/01/2016 03:31:33.

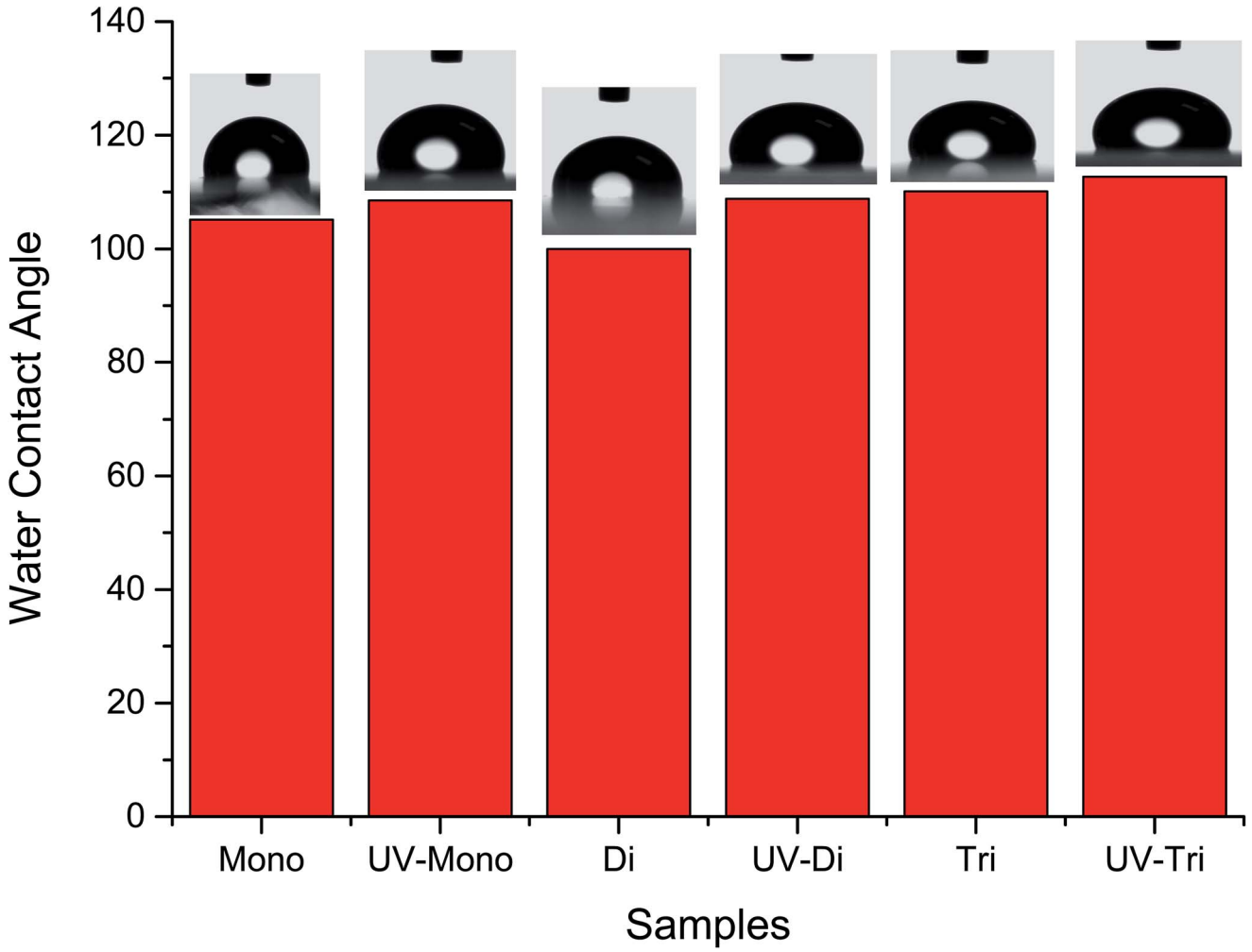


Fig. 11 WCAs of poly(mono-coumarin BZ), poly(di-coumarin BZ), and poly(tri-coumarin BZ) prepared through thermal curing at 210 °C before and after UV exposure at 365 nm.

**Water contact angles of photocrosslinked coumarin-functionalized PBZs**

The physical properties of PBZs are dependent on the degrees of intra- and intermolecular hydrogen bonding between the phenolic OH groups and the N atoms in the Mannich bridges after ring opening of the benzoxazine monomers.[18,21] In this present study, we observed evidence, using FTIR spectroscopy, for additional intramolecular OH···O═C hydrogen bonding between the C═O groups of the coumarin units and the OH groups. Fig. 11 and S6† summarize the WCAs for poly(mono-coumarin BZ), poly(di-coumarin BZ), and poly(tri-coumarin BZ) before and after photodimerization and then thermal polymerization at 210 °C for 2 h, and after applying different thermal curing conditions (Fig. S9†), respectively. Interestingly, the WCAs of the poly(mono-coumarin BZ), poly(di-coumarin BZ), and poly(tri-coumarin BZ) polymers obtained after photodimerization of the coumarin units of their monomers and subsequent thermal curing were 108, 108, and 122°, respectively; they were higher than those of the poly(mono-coumarin BZ), poly(di-coumarin BZ), and poly(tri-coumarin BZ) polymers obtained after thermal curing alone (105, 100, and 110°, respectively). In addition, the WCA values of the poly(tri-coumarin BZ) obtained after both photodimerization and thermal curing was higher than those of the corresponding poly(mono-coumarin BZ) and poly(di-coumarin BZ) polymers, due to greater intramolecular OH···N hydrogen bonding (from the Mannich bridges) and additional intramolecular OH···O═C hydrogen bonding (between the C═O groups of the coumarin units and the phenolic OH groups) of the poly(tri-coumarin BZ).

## Conclusions

We have synthesized three different photo-crosslinkable coumarin-containing benzoxazine monomers through facile Mannich reactions of coumarin–OH and paraformaldehyde with aniline, bisphenol A–$NH_2$, and 1,3,5-tri(4-aminophenoxy) benzene, respectively, in 1,4-dioxane. FTIR, NMR and high resolution mass spectra confirmed the chemical structures of these three benzoxazine monomers. DSC and TGA analyses revealed that the glass transition temperatures, thermal decomposition temperatures, and char yields of the resulting polymers were strongly dependent on the valency of the

 This journal is © The Royal Society of Chemistry 2016

Published on 21 January 2016. Downloaded by Universitaet Osnabrueck on 29/01/2016 03:31:33.

monomers and the degrees of photodimerization of the coumarin units, both of which affected the crosslinking densities. In addition, the WCAs of the poly(tri-coumarin BZ) polymers obtained with and without photodimerization possessed highly hydrophobic surfaces because strong intramolecular hydrogen bonding; these highly thermally stable and highly hydrophobic surfaces could be good candidates for use in high-performance applications and polymer coatings.

## Acknowledgements

This study was supported financially by the Ministry of Science and Technology, Taiwan, Republic of China, under contracts MOST103-2221-E-110-079-MY3 and MOST102-2221-E-110-008-MY3.

## References

1 H. Ishida and Y. Rodriguez, *Polymer*, 1995, **36**, 3151–3158.
2 N. N. Ghosh, B. Kiskan and Y. Yagci, *Prog. Polym. Sci.*, 2007, **32**, 1344–1391.
3 Y. X. Wang and H. Ishida, *Polymer*, 1999, **40**, 4563–4570.
4 (*a*) M. G. Mohamed, W. C. Su, Y. C. Lin, C. F. Wang, J. K. Chen, K. U. Jeong and S. W. Kuo, *RSC Adv.*, 2014, **4**, 50373–50385; (*b*) C. Liu, D. Shen, R. M. Sebastián, J. Marquet and R. Schönfeld, *Polymer*, 2013, **54**, 2873–2878.
5 (*a*) W. H. Hu, K. W. Huang and S. W. Kuo, *Polym. Chem.*, 2012, **3**, 1546–1554; (*b*) J. Sun, W. Wei, Y. Xu, X. D. Liu and T. Endo, *RSC Adv.*, 2015, **5**, 19048–19054; (*c*) F. Meng, H. Ishida and X. Liu, *RSC Adv.*, 2014, **4**, 9471–9475; (*d*) M. G. Mohamed, C. H. Hsiao, F. Luo, L. Dai and S. W. Kuo, *RSC Adv.*, 2015, **5**, 45201–45212.
6 (*a*) S. W. Kuo, Y. C. Wu, C. F. Wang and K. U. Jeong, *J. Phys. Chem. C*, 2009, **113**, 20666–20673; (*b*) K. Zhang and H. Ishida, *Polym. Chem.*, 2015, **6**, 2541–2550; (*c*) S. Ohashi, J. Kilbane, T. Herl and H. Ishida, *Macromolecules*, 2015, **48**, 8412–8417.
7 L. Qu and Z. Xin, *Langmuir*, 2011, **27**, 8365–8370.
8 A. Sudo, R. Kudoh, H. Nakayama, K. Arima and T. Endo, *Macromolecules*, 2008, **41**, 9030–9034.
9 Y. J. Lee, S. W. Kuo, C. F. Huang and F. C. Chang, *Polymer*, 2006, **47**, 4378–4386.
10 M. A. Tasdelen, B. Kiskan and Y. Yagci, *Macromol. Rapid Commun.*, 2006, **27**, 1539–1544.
11 M. R. Vengatesan, S. Devaraju, K. Dinakaran and M. Alagar, *J. Mater. Chem.*, 2012, **22**, 7559.
12 Y. Yagci, B. Kiskan and N. N. Ghosh, *J. Polym. Sci., Part A: Polym. Chem.*, 2009, **47**, 5565–5576.
13 C. F. Wang, Y. C. Su, S. W. Kuo, C. F. Huang, Y. C. Sheen and F. C. Chang, *Angew. Chem., Int. Ed.*, 2006, **45**, 2248–2251.
14 (*a*) M. Imran, B. Kiskan and Y. Yagci, *Tetrahedron Lett.*, 2013, **54**, 4966–4969; (*b*) J. Wu, Y. Xi, G. T. McCandless, Y. Xie, R. Menon, Y. Patel, D. J. Yang, S. T. Lacono and B. M. Novak, *Macromolecules*, 2015, **48**, 6087–6095.
15 T. Takeichi, T. Kano and T. Agag, *Polymer*, 2005, **46**, 12172–12180.
16 (*a*) J. L. Shi, X. S. Zheng, L. P. Xie, F. F. Cao, Y. Wu and W. B. Liu, *Eur. Polym. J.*, 2013, **49**, 4054–4061; (*b*) M. Arslan, B. Kiskan and Y. Yagci, *Macromolecules*, 2015, **48**, 1329–1334.
17 C. F. Wang, S. F. Chiou, F. H. Ko, J. K. Chen, C. T. Chou, C. F. Huang, S. W. Kuo and F. C. Chang, *Langmuir*, 2007, **23**, 5868–5871.
18 C. F. Wang, F. C. Chang and S. W. Kuo, in *Handbook of Benzoxazine Resins*, ed. H. Ishida and T. Agag, Elsevier, Amsterdam, 2011, ch. 33, p. 579.
19 M. R. Vengatesan, S. Devaraju, K. Dinakaran and M. Alagar, *J. Mater. Chem.*, 2012, **22**, 7559–7566.
20 A. Sudo, R. Kudoh, H. Nakayama, K. Arima and T. Endo, *Macromolecules*, 2008, **41**, 9030–9034.
21 H. Ishida, in *Handbook of Benzoxazine Resins*, ed. H. Ishida and T. Agag, Elsevier, Amsterdam, 2011, ch. 1, p. 1.
22 N. Gogoi, D. Rastogi, M. Jassal and A. K. Agrawal, *J. Text. Inst.*, 2014, **105**, 1212–1220.
23 (*a*) J. Jiang, X. Tong and Y. Zhao, *J. Am. Chem. Soc.*, 2005, **127**, 8290–8291; (*b*) K. Gnanaguru, N. Ramasubbu, K. Venkatesan and V. Ramamurthy, *J. Org. Chem.*, 1985, **50**, 2337–2346; (*c*) X. Yu, D. Scheller, O. Rademacher and T. Wolff, *J. Org. Chem.*, 2003, **68**, 7388–7399.
24 (*a*) G. Liu and C. M. Dong, *Biomacromolecules*, 2012, **13**, 1573–1583; (*b*) T. Wolff and H. Gorner, *Phys. Chem. Chem. Phys.*, 2004, **6**, 368–376.
25 R. J. Dong, B. S. Zhu, Y. F. Zhou, D. Y. Yan and X. Y. Zhu, *Polym. Chem.*, 2013, **4**, 912–915.
26 (*a*) Y. Huang, R. Dong, X. Zhu and D. Yan, *Soft Matter*, 2014, **10**, 6121–6138; (*b*) K. Tanaka, *Molecules*, 2012, **17**, 1408–1418.
27 S. R. Trenor, A. R. Shultz, B. J. Love and T. E. Long, *Chem. Rev.*, 2004, **104**, 3059–3077.
28 (*a*) M. Nagata and Y. Yamamoto, *React. Funct. Polym.*, 2008, **68**, 915–921; (*b*) M. V. S. N. Maddipatla, D. Wehrung, C. Tang, W. Fan, M. O. Oyewumi, T. Miyoshi and A. Toy, *Macromolecules*, 3013, **46**, 5133–5140; (*c*) B. Kiskan and Y. Yagci, *J. Polym. Sci., Part A: Polym. Chem.*, 2014, **52**, 2911–2918.
29 Y. Chujo, K. Sada and T. Saegusa, *Macromolecules*, 1990, **23**, 2693–2697.
30 B. Kiskan and Y. Yagci, *J. Polym. Sci., Part A: Polym. Chem.*, 2007, **45**, 1670–1676.
31 (*a*) M. G. Mohamed, K. C. Hsu and S. W. Kuo, *Polym. Chem.*, 2015, **6**, 2423–2433; (*b*) C. R. Arza, P. Froimowicz and H. Ishida, *RSC Adv.*, 2015, **5**, 97855–97861; (*c*) M. Comi, G. Lligades, J. C. Ronda, M. Galia and V. Cadiz, *J. Polym. Sci., Part A: Polym. Chem.*, 2013, **51**, 4894–4903.
32 H. Ishida and S. Ohba, *Polymer*, 2005, **46**, 5588–5595.
33 (*a*) A. Chernykh, T. Agag and H. Ishida, *Polymer*, 2009, **50**, 3153–3157; (*b*) T. Agag and T. Takeichi, *Macromolecules*, 2001, **34**, 7257–7263; (*c*) T. Agag and T. Takeichi, *Macromolecules*, 2003, **36**, 6010–6017; (*d*) B. Kiskan and Y. Yagci, *Polymer*, 2008, **49**, 2455–2460; (*e*) B. Kiskan, B. Aydogan and Y. Yagci, *J. Polym. Sci., Part A: Polym. Chem.*, 2009, **47**, 804–811; (*f*) A. Chernykh, T. Agag and H. Ishida, *Macromolecules*, 2009, **42**, 5121–5127; (*g*) S. W. Kuo and W. C. Liu, *J. Appl. Polym. Sci.*, 2010, **117**, 3121–3127.

34 Y. C. Su, S. W. Kuo, D. R. Yei, H. Xu and F. C. Chang, *Polymer*, 2003, **44**, 2187–2191.
35 P. Phiriyawirut, R. Magaraphan and H. Ishida, *Mater. Res. Innovations*, 2001, **4**, 187–196.
36 W. H. Hu, K. W. Huang, C. W. Chiou and S. W. Kuo, *Macromolecules*, 2012, **45**, 9020–9028.
37 C. C. Yang, Y. C. Lin, P. I. Wang, D. J. Liaw and S. W. Kuo, *Polymer*, 2014, **55**, 2044–2050.
38 Y. L. Liu and T. W. Chuo, *Polym. Chem.*, 2013, **4**, 2194–2205.
39 B. Kiskan and Y. Yagci, *J. Polym. Sci., Part A: Polym. Chem.*, 2014, **52**, 2911–2918.
40 D. Kehrlösser, J. Träger, H. C. Kim and N. Hampp, *Langmuir*, 2010, **26**, 3878–3882.
41 T. A. Moore, M. L. Harter and P. S. Song, *J. Mol. Spectrosc.*, 1971, **40**, 144–157.

Published on 21 January 2016. Downloaded by Universitaet Osnabrueck on 29/01/2016 03:31:33.


This journal is © The Royal Society of Chemistry 2016